

The Distance, Inclination, and Spin of the Black Hole Microquasar H1743–322

James F. Steiner¹, Jeffrey E. McClintock¹, and Mark J. Reid¹

jsteiner@cfa.harvard.edu

ABSTRACT

During its 2003 outburst, the black-hole X-ray transient H1743–322 produced two-sided radio and X-ray jets. Applying a simple and symmetric kinematic model to the trajectories of these jets, we determine the source distance, 8.5 ± 0.8 kpc, and the inclination angle of the jets, $75^\circ \pm 3^\circ$. Using these values, we estimate the spin of the black hole by fitting its *RXTE* spectra, obtained during the 2003 outburst, to a standard relativistic accretion-disk model. For its spin, we find $a_* = 0.2 \pm 0.3$ (68% limits); $-0.3 < a_* < 0.7$ at 90% confidence. We rule strongly against an extreme value of spin: $a_* < 0.92$ at 99.7% confidence. H1743–322 is the third known microquasar (after A0620–00 and XTE J1550–564) that displays large-scale ballistic jets and has a moderate value of spin. Our result, which depends on an empirical distribution of black hole masses, takes into account all known sources of measurement error.

Subject headings: black hole physics — stars: individual (H1743–322) — X-rays: binaries

1. Introduction

About 50 stellar-mass black holes have been discovered and about two dozen of these have been well studied at optical or radio wavelengths (Remillard & McClintock 2006; Özel et al. 2010). They are all accretion-powered X-ray sources located in X-ray binary systems. In each system, the X-ray source is fueled by gas that feeds from a mass-donor star into the black hole’s accretion disk. Within a few hundred kilometers of the black hole, the gas reaches a temperature of $\sim 10^7$ K and produces a luminosity that can approach the Eddington limit ($\sim 10^{39}$ erg s^{−1}). More than 80% of such sources are transient, with outbursts lasting a

¹Harvard-Smithsonian Center for Astrophysics, 60 Garden Street, Cambridge, MA 02138.

year or so followed by years or decades of quiescence. Typically, the host binaries have short orbital periods ($P \sim 1$ day) and are comprised of a low-mass ($\lesssim 1 M_\odot$) secondary star and a $\sim 10 M_\odot$ black hole. Presently, neither the masses nor the orbital period of our featured system, H1743–322, are known. Nevertheless, as we now describe, the wealth of data available for H1743–322 (hereafter H1743) strongly indicates that it is a typical short-period black hole transient.

Studies of X-ray spectral and timing data leave little doubt that H1743 contains a black hole primary (Kalemci et al. 2006; McClintock et al. 2009; Motta et al. 2010), notwithstanding the lack of dynamical evidence. While large outbursts of H1743 occurred in 1977, 2003 and 2008, our focus here is on the major 2003 outburst. During this 9-month active period, H1743 was observed 170 times using the PCA and HEXTE detectors aboard the *Rossi X-ray Timing Explorer (RXTE)* (McClintock et al. 2009). The source exhibited two distinct phases of evolution: (1) During the first three months (when the source was observed on an almost daily basis) H1743 flared continually and violently and was in the steep power-law (SPL) or intermediate (SPL:Hard) state (see Remillard & McClintock for discussion of these X-ray states). On the 47th day of outburst (MJD 52766), an event of central importance occurred – the radio/X-ray jets we model were launched during an intense power-law flare (discussed below). (2) During the next four months, the source was locked in the thermal dominant (TD) state, and the source intensity decayed smoothly and monotonically. It is primarily these TD-state data that we use to determine the spin of H1743.

An important X-ray timing result derived from the 2003 outburst was the discovery of a pair of quasi-periodic oscillations (QPOs) at 240 Hz and 165 Hz (Homan et al. 2005; Remillard et al. 2006). Similar high-frequency (HF) QPOs with a commensurate frequency ratio of 3:2 are seen for three other dynamically-confirmed black holes (XTE J1550–564, GRO J1655–40 and GRS 1915+105).

About one year after the onset of the 2003 outburst, bipolar X-ray jets were discovered and observed a total of three times using *Chandra* (Corbel et al. 2005). Radio observations, which commenced several months before the X-ray observations, resulted in four detections of the eastern jet (only), followed about two months later by a single detection of the western jet (Corbel et al. 2005). Large-scale X-ray jets are rare, having been previously observed for only one other microquasar, namely XTE J1550–564, which is similar in many respects to H1743 (for comparisons, see McClintock et al. 2009). In its 1998 outburst, XTE J1550–564 produced relativistic jets at early times whose launch date was unambiguously tied to the occurrence of a remarkable X-ray flare (Hannikainen et al. 2009; Steiner & McClintock 2012).

H1743’s X-flare on MJD 52766 showed striking similarities to the giant flare of XTE

J1550–564 (see Figure 12 of McClintock et al. 2009). Of particular note, both flares occurred during a dip in the X-ray rms power (0.1–10 Hz), a jump in frequency of the low-frequency QPOs, onset of the high-frequency QPOs, and the apex of power-law emission (Sobczak et al. 2000; Remillard et al. 2006). The similar character of these two flares, and the coincidence for XTE J1550–564 between the X-ray flare and the launch date of the jets, motivated us to search the VLA archive for additional observations of H1743. This search was fruitful, and in Section 2 we report three additional radio jet detections at early times that link the jets to the 2003 X-ray flare.

To deduce the source distance and jet inclination angle of H1743, we model the proper-motion data derived from the X-ray and radio observations. In doing so, we closely follow our recent study of the large-scale X-ray/radio jets of XTE J1550–564 (Steiner & McClintock 2012), which builds on the pioneering work of Wang et al. (2003) and Hao & Zhang (2009). Using a model originally applied to gamma-ray bursts, we concluded that XTE J1550–564 is embedded in a pc-scale cavity in which the jets expanded unimpeded until they impacted the cavity walls and rapidly decelerated. We apply this same model to H1743 and obtain constraints on the distance and jet inclination angle (presumed to be the inclination of the spin axis; see Steiner & McClintock 2012).

The evolution of H1743’s jets have already been studied by Hao & Zhang (2009); however, our aims differ from theirs. They were primarily interested in the environment of the black hole. While assuming an earlier launch date for the jets, they adopted the nominal values of distance and inclination ($D = 8$ kpc and $i = 73^\circ$) suggested by Corbel et al. (2005). Our attention is focused on deriving accurate constraints on D and i for H1743, which we use in turn to constrain the spin of the black hole¹.

We measure the spin of H1743 using the continuum-fitting (CF) method (McClintock et al. 2011; Zhang et al. 1997). In the CF method, one estimates the inner radius of the accretion disk R_{in} , which is identified with the radius of the innermost stable circular orbit R_{ISCO} . Knowing both R_{ISCO} and M is equivalent to knowing the spin parameter a_* because R_{ISCO}/M is a monotonic function of a_* , decreasing from 6 to 1 as the spin parameter increases from 0 to 1 (Bardeen et al. 1972)². In the CF method, one determines R_{ISCO} by modeling the X-ray continuum spectrum of the dominant thermal component using a fully relativistic model of a thin accretion disk. The observables are X-ray flux, temperature, distance D , inclination i , and mass M . In order to obtain reliable values of a_* , it is essential to select X-ray spectra

¹We express black hole spin in the customary way as the dimensionless quantity $a_* \equiv cJ/GM^2$ with $|a_*| \leq 1$, where M and J are respectively the black hole mass and angular momentum.

²Using $c = G = 1$.

that have a strong thermal component and to have accurate estimates of D , i , and M . For H1743, we use our jet model to determine the first two parameters, and we constrain M using the known distribution of black hole masses for X-ray transient sources.

2. Data

To search for the presence of radio jets near the time of their expected production (Section 1), we examined high spatial resolution A-configuration VLA images taken early during H1743’s 2003 outburst (see McClintock et al. 2009). Calibrated data from the VLA archive for program AR523 on MJD 52779.4, 52782.4, and 52786.4 were imaged using the Astronomical Image Processing System (AIPS) task IMAGR. The source was detected at 8.4 and 14.9 GHz, but here we only use the 14.9 GHz data, which had sufficient angular resolution to clearly resolve source components. The synthesized beam was approximately $0.6''$ by $0.2''$ elongated north-south. Fortunately, the jet position angle is almost exactly east-west (Corbel et al. 2005), allowing us to identify components separated by $\gtrsim 0.2''$. At all three epochs, the source displayed a dominant component and a weak component offset towards the west. At MJD 52779.4, just 13 days after H1743’s X-ray flare, their separation was 166 ± 20 mas. Later, on MJD 52782.4 and MJD 52786.4 the separations were 256 ± 20 mas and 288 ± 20 mas, respectively.

The majority of the jet data considered in our analysis are taken from Tables 1 and 3 of Corbel et al. (2005). These tables provide jet-source separation measurements for radio and X-ray observations which were conducted from 6 months onward following H1743’s jet-launching flare. The X-ray data consist of three ~ 30 ks *Chandra* X-ray observations in which both jets were detected. In radio, Corbel et al. (2005) report on five observations from the Australian Telescope Compact Array (ATCA). The eastern jet was present in each image, but the western jet was detected only in the final observation. These X-ray and radio observations were carried out between MJD 52955 and MJD 53092, when the jet-source separations were in the range $\sim 4'' - 7''$. The substantially larger angular separations of the eastern jet indicate that it is approaching and the western jet is receding.

In determining the spin of H1743, we analyze the full set of *RXTE* PCU-2 “standard 2” data obtained during the 2003 outburst, with the spectra binned into 170 half-day intervals. These spectra have been modeled in detail by McClintock et al. (2009) and Steiner et al. (2009), and we use the same data reduction procedures here. Briefly, all the data are dead-time corrected, background subtracted, and analyzed with the inclusion of a 1% systematic uncertainty (Jahoda et al. 2006). We standardize all detector calibrations to the Toor & Seward (1974) values for the Crab using a custom model which adjusts both the

overall flux normalization and the spectral shape (see Steiner et al. 2010). During the early weeks of the outburst cycle, *RXTE*’s pointing was offset by 0.32° from H1743. We have corrected the fluxes to the full collimator transmission by assuming a triangular response with $\text{FWHM} = 1^\circ$ (see Steiner et al. 2009).

3. The Ballistic Jets: Model and Results

Our jet model, which is based on one developed by Wang et al. (2003), was first applied in describing gamma-ray-bursts. Here, we consider a pair of symmetric jets, each ejected with an initial kinetic energy E_0 and Lorentz factor Γ_0 . During their expansion, the jets decelerate as they sweep up gas in their paths. Assuming adiabatic expansion, the evolution of each jet is governed by:

$$E_0 = (\Gamma - 1)M_0c^2 + \sigma(\Gamma_{\text{sh}}^2 - 1)m_{\text{sw}}c^2, \quad (1)$$

where Γ is the bulk Lorentz factor of the jet, M_0 the mass of the ejecta, σ is a numerical factor of order unity³, and Γ_{sh} is the Lorentz factor of randomly accelerated particles at the shock front. The entrained mass, m_{sw} , is given by $m_{\text{sw}} = \Theta^2 m_p n \pi R^3 / 3$, where Θ is the jet half opening angle, n the gas density, m_p is the mass of a proton, and R the distance traveled by the jet.

We evolve Eqn. 1 in 2-hour time steps, using the inclination of the jet axis to the observer’s line of sight (θ) to calculate the projected separation (δ) between each jet and the central source: $\delta(t') = R(t) \sin \theta / D$. Here, $t' = t \pm R(t) \cos \theta / c$ is the observer’s time, which takes into account for each jet the time delay between H1743’s rest frame and the frame of the observer.

Our full model requires just five parameters: D , θ , Γ_0 , the launch date T_0 , and \tilde{E} , the effective energy⁴. Because of the association with the X-ray flare, the prior on the launch date is taken to be $\text{MJD } 52766 \pm 5$ days; we adopt a flat prior on θ , D , $\log(\Gamma_0)$, and $\log(\tilde{E})$. Our model is fitted via a Markov chain Monte Carlo (MCMC) routine developed using the Metropolis-Hastings algorithm (Hastings 1970) which has been previously applied with this jet model in Steiner & McClintock (2012). The chains are evolved until they are well

³ σ ranges from 0.35 in the ultrarelativistic limit to 0.73 in the nonrelativistic limit. For additional details concerning our model, see Steiner & McClintock (2012).

⁴ $\tilde{E} \equiv E_0(n/10^{-2}\text{cm}^{-3})^{-1}(\Theta/1^\circ)^{-2}$. Following our approach for XTE J1550–564 (Steiner & McClintock 2012), we scale Θ and n using typical values, with density 100 times lower than for the interstellar medium.

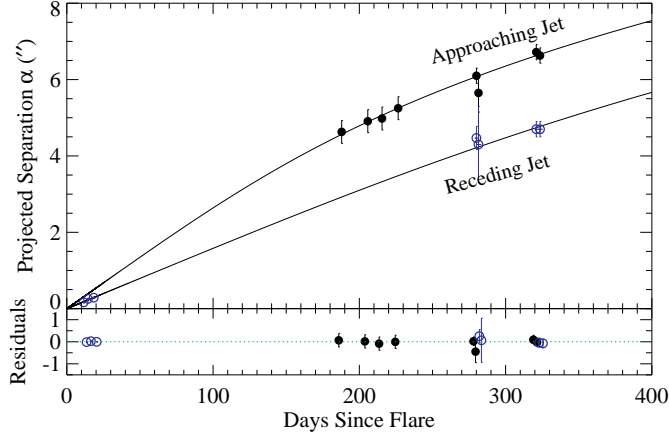


Fig. 1.— Our best fit model for the motion of H1743’s radio and X-ray jets. The eastern jet is marked by filled circles and the western jet by open circles. Fit residuals are shown in the bottom panel using a slight offset in time between eastern and western jets.

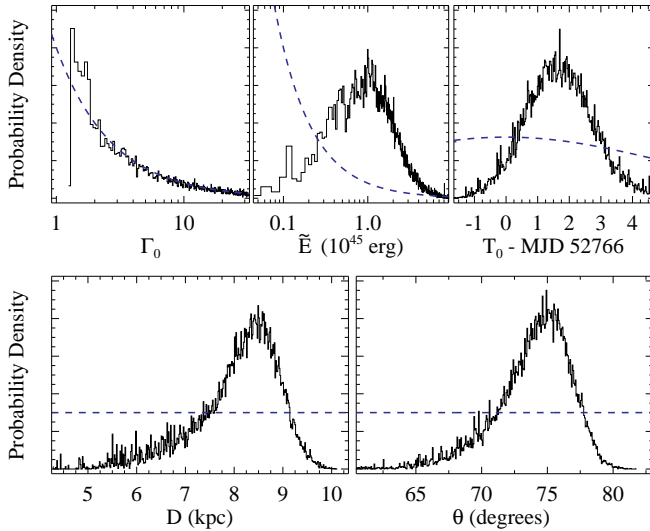


Fig. 2.— Marginalized probability densities from the MCMC model are shown to arbitrary scale. The prior for each parameter is indicated by a dashed line. Γ_0 is constrained by its prior at large values, but the other parameters show little dependence on their priors.

converged, using $\sim 2 \times 10^5$ elements total⁵.

From the VLA data alone, the identification of the pair of radio sources is ambiguous. We have applied our model by attributing to the two radio sources each allowed combination of eastern jet, western jet, and core. The most probable interpretation is that the two sources correspond to emission from the core and the western jet. Alternative pairings are ruled out at $> 97\%$ confidence by our model.

The best fit achieved by the MCMC run is shown in Figure 1 and reaches a goodness of fit $\chi^2/\nu = 4.9/9 = 0.54$. Obviously, further modification to the model is not needed⁶. Distributions for the model parameters are shown in Figure 2. Of chief importance, we find that distance and inclination are well constrained: $D = 8.5 \pm 0.8$ kpc and $i = 75^\circ \pm 3^\circ$. This distance places H1743 near the Galactic center, which is expected, given its projected separation of only $\approx 2^\circ$ from the Galactic center. The time at which the jets were produced is constrained to $T_0 = \text{MJD } 52767.6 \pm 1.1$ days, independent of the prior. This timing supports a connection between H1743’s X-ray flare and the production of its jets. The speed of the jets, Γ_0 , has a relatively low maximum a posteriori estimate, $\Gamma_0 \sim 1.4$, but is poorly constrained at high values and tracks its prior. For the kinematic energy of each jet, we obtain a large uncertainty of ≈ 0.5 dex centered around $\tilde{E} \approx 10^{45}$ erg. This implies that H1743’s jets are only about a tenth as energetic as those produced in the 1998 outburst of XTE J1550–564 or, alternatively, for H1743 either (1) the density of the surrounding medium is much lower or (2) the jet opening angle is substantially smaller.

4. X-ray Continuum-Fitting Analysis

We now estimate the spin of H1743 by fitting its X-ray spectra. For the three crucial input parameters, we use the values of D and i derived in the preceding section and the distribution of black hole masses discussed below. All of our analysis is performed using XSPEC v12.7.0 (Arnaud 1996). Following Steiner et al. (2009) and making minor adjustments, our spectral model has the form $\text{TBABS}(\text{SIMPL} \otimes \text{KERRBB2})$, where TBABS and KERRBB2 are, respectively, the low-energy-absorption and accretion-disk components. The component SIMPL scatters a fraction of the thermal disk photons into a Compton power law. For H1743, this simple convolution model describes only the broad continuum components

⁵An additional $\approx 10^5$ chain elements, which were generated during training and burn-in phases, were not used.

⁶We have explored the asymmetric models employed for XTE J1550–564 (Steiner & McClintock 2012); i and D are unchanged.

and is unaffected by the inclusion of weaker features due, e.g., to warm absorbers or spectral reflection.

The four free parameters of the spectral model⁷ are the (1) fraction of thermal photons f_{SC} scattered into the Compton power law; (2) power-law index Γ ; (3) spin parameter a_* ; and mass accretion rate \dot{M} . Mass, inclination, and distance are varied in 5×10^3 Monte-Carlo samples, and all 170 spectra are fitted for each setting. Uncertainty in the absolute calibration of the X-ray flux is accounted for by randomly varying the overall flux normalization by 10% for each triplet setting of M , i , and D (e.g., Steiner et al. 2011). We similarly marginalize over uncertainty in the viscosity parameter α by randomly assigning either $\alpha = 0.01$ or $\alpha = 0.1$ (e.g., King et al. 2007; Pessah et al. 2007), which are two representative values available to our model. Both of these uncertainties have a small effect on a_* compared to our dominant uncertainty, the unknown black hole mass. (Uncertainty in the mass accounts for 50% of our final uncertainty in a_* .)

For each of the 5×10^3 parameter settings, we apply our standard data selection criteria: disk luminosity between 3% and 30% of the Eddington limit; goodness of fit $\chi^2/\nu < 2$; and a power-law normalization $f_{\text{SC}} < 25\%$ (Steiner et al. 2009). Typically, about 30 spectra pass this screening. Finally, each of the 5×10^3 samples is given a weight according to the mass distribution assumed, and random draws are made from the selected spectra to achieve an estimate of spin. The dependence between the inferred value of spin and the black hole’s mass is illustrated in Figure 3. As mass is varied from $M = 5M_\odot$ to $15M_\odot$, spin changes from $a_* \approx -0.25$ to $a_* \approx 0.75$.

Recently, Özel et al. (2010) compiled all the dynamical measurements of mass for black hole transients and determined the following best-fit probability distribution, which we adopt:

$$P(M) = \begin{cases} \text{Exp}[(6.30M_\odot - M)/1.57M_\odot]/1.57M_\odot, & M > 6.3M_\odot, \\ 0, & M \leq 6.3M_\odot. \end{cases} \quad (2)$$

In Figure 4, we show the spin which results when the Özel et al. (2010) mass distribution is assumed. We find $a_* = 0.20^{+0.34}_{-0.33}$ (68% confidence interval) with a 90% confidence interval of $-0.33 < a_* < 0.70$. We also find that extreme values of spin are ruled out; $a_* < 0.92$ at 99.7% confidence. This makes H1743 one of a growing population of black hole microquasars known to have moderate spin (e.g., A0620–00, $a_* \approx 0.1$; Gou et al. 2010, XTE J1550–564,

⁷Column density N_{H} is frozen at $2.0 \times 10^{22} \text{ cm}^{-2}$ (Blum et al. 2009). For KERRBB2, limb darkening and returning radiation are switched on and the torque at the inner boundary is set to zero. For SIMPL, we use the faster upscattering-only option.

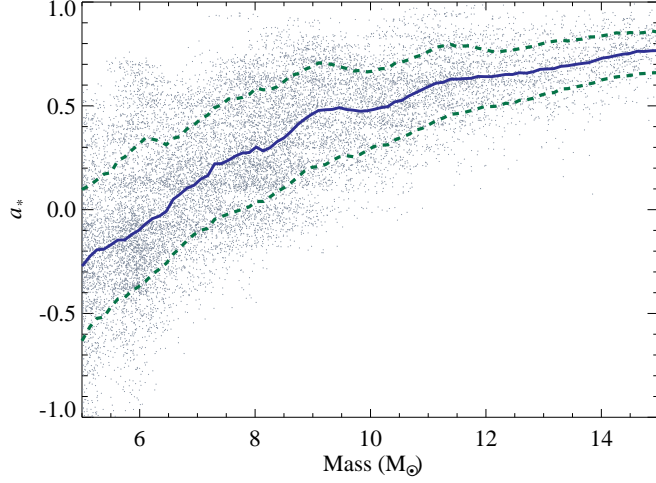


Fig. 3.— The dependence of spin on black hole mass. These estimates incorporate all sources of measurement error. The solid line tracks the average spin at each mass, and the associated 68% confidence interval corresponds to the region between dashed lines.

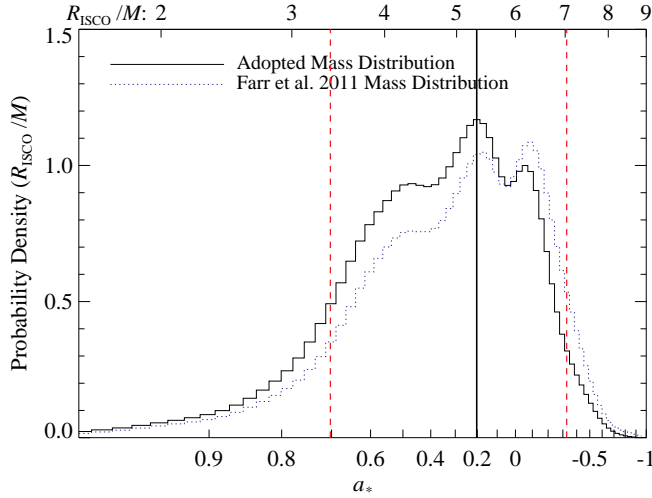


Fig. 4.— Spin probability for the dimensionless measurement variable R_{ISCO}/M (top axis) which uniquely determines the spin parameter a_* (bottom axis). This spin estimate is obtained by using the adopted transient black hole mass distribution from Özel et al. (2010) (solid curve). The vertical solid line indicates the maximum likelihood spin, while the 90% confidence range is bounded by dashed vertical lines. For comparison, we also show the spin estimate from using the mass distribution of Farr et al. (2011) (dotted curve). These results take into account uncertainties in M , i , D , α and the absolute X-ray flux calibration. For illustration, the distributions over R_{ISCO}/M have been smoothed using a Gaussian kernel with 10% width.

$a_* \approx 0.5$; Steiner et al. 2011).

In Figure 4, we also show results using the mass distribution favored by Farr et al. (2011). These authors and Özel et al. (2010) used the same black-hole mass data, but Farr et al. found that a power-law distribution gave the best fit, with form $P(M) \propto M^{-6.4}$ over the mass range $6.1M_\odot \leq M \leq 23M_\odot$ (and $P(M) = 0$ elsewhere). Comparing the Farr et al. distribution with our adopted result, we find that the difference is minor: $\Delta a_* \approx 0.05$.

5. Conclusions

We have modeled the proper motion of the radio and X-ray jets of H1743 that were launched during an X-ray flare. Based on our purely kinematic model, we obtain firm estimates of the source distance, 8.5 ± 0.8 kpc, and the jet inclination angle, $75^\circ \pm 3^\circ$. Using these constraints on D and i , we fitted all 170 X-ray spectra collected during the 2003 outburst of H1743, applied our data selection criteria, and derived a relationship between spin and black hole mass. We then constrained the mass of H1743 using an analytic distribution for transient systems that are similar to H1743, thereby arriving at our final result: $a_* = 0.2 \pm 0.3$ ($-0.3 < a_* < 0.7$ at 90% confidence). Meanwhile, we rule strongly against an extreme value of spin: $a_* < 0.92$ at 99.7% confidence. Two similar microquasars have been identified which also produced powerful jets while harboring black holes with moderate spins: A0620–00 ($a_* \approx 0.1$; Gou et al. 2010) and J1550–564 ($a_* \approx 0.5$; Steiner et al. 2011).

This is the first successful application of the X-ray continuum-fitting method that does not rely on any dynamical data to place constraints on one or more of the input parameters D , M and i – even the orbital period of H1743 is presently unknown! Our constraint on a_* can be tightened once a dynamical estimate of mass has been obtained.

JFS was supported by the Smithsonian Institution Endowment Funds and JEM acknowledges support from NASA grant NNX11AD08G. Computations were performed using the Odyssey cluster which is supported by the FAS Science Division Research Computing Group at Harvard University.

Facilities: VLA, RXTE, Chandra

REFERENCES

- Arnaud, K. A. 1996, in *Astronomical Society of the Pacific Conference Series*, Vol. 101, *Astronomical Data Analysis Software and Systems V*, ed. G. H. Jacoby & J. Barnes, 17
- Bardeen, J. M., Press, W. H., & Teukolsky, S. A. 1972, *ApJ*, 178, 347
- Blum, J. L., Miller, J. M., Fabian, A. C., Miller, M. C., Homan, J., van der Klis, M., Cackett, E. M., & Reis, R. C. 2009, *ApJ*, 706, 60
- Corbel, S., Kaaret, P., Fender, R. P., Tzioumis, A. K., Tomsick, J. A., & Orosz, J. A. 2005, *ApJ*, 632, 504
- Farr, W. M., Sravan, N., Cantrell, A., Kreidberg, L., Bailyn, C. D., Mandel, I., & Kalogera, V. 2011, *ApJ*, 741, 103
- Gou, L., McClintock, J. E., Steiner, J. F., Narayan, R., Cantrell, A. G., Bailyn, C. D., & Orosz, J. A. 2010, *ApJ*, 718, L122
- Hannikainen, D. C., et al. 2009, *MNRAS*, 397, 569
- Hao, J. F., & Zhang, S. N. 2009, *ApJ*, 702, 1648
- Hastings, W. 1970, *Biometrika*, 97
- Homan, J., Miller, J. M., Wijnands, R., van der Klis, M., Belloni, T., Steeghs, D., & Lewin, W. H. G. 2005, *ApJ*, 623, 383
- Jahoda, K., Markwardt, C. B., Radeva, Y., Rots, A. H., Stark, M. J., Swank, J. H., Strohmayer, T. E., & Zhang, W. 2006, *ApJS*, 163, 401
- Kalemci, E., Tomsick, J. A., Rothschild, R. E., Pottschmidt, K., Corbel, S., & Kaaret, P. 2006, *ApJ*, 639, 340
- King, A. R., Pringle, J. E., & Livio, M. 2007, *MNRAS*, 376, 1740
- McClintock, J. E., et al. 2011, *Classical and Quantum Gravity*, 28, 114009
- McClintock, J. E., Remillard, R. A., Rupen, M. P., Torres, M. A. P., Steeghs, D., Levine, A. M., & Orosz, J. A. 2009, *ApJ*, 698, 1398
- Motta, S., Muñoz-Darias, T., & Belloni, T. 2010, *MNRAS*, 408, 1796
- Özel, F., Psaltis, D., Narayan, R., & McClintock, J. E. 2010, *ApJ*, 725, 1918

- Pessah, M. E., Chan, C.-k., & Psaltis, D. 2007, *ApJ*, 668, L51
- Remillard, R. A., & McClintock, J. E. 2006, *ARA&A*, 44, 49
- Remillard, R. A., McClintock, J. E., Orosz, J. A., & Levine, A. M. 2006, *ApJ*, 637, 1002
- Sobczak, G. J., McClintock, J. E., Remillard, R. A., Cui, W., Levine, A. M., Morgan, E. H., Orosz, J. A., & Bailyn, C. D. 2000, *ApJ*, 531, 537
- Steiner, J. F., & McClintock, J. E. 2012, *ApJ*, in press
- Steiner, J. F., McClintock, J. E., Remillard, R. A., Gou, L., Yamada, S., & Narayan, R. 2010, *ApJ*, 718, L117
- Steiner, J. F., McClintock, J. E., Remillard, R. A., Narayan, R., & Gou, L. J. 2009, *ApJ*, 701, L83
- Steiner, J. F., et al. 2011, *MNRAS*, 416, 941
- Toor, A., & Seward, F. D. 1974, *AJ*, 79, 995
- Wang, X. Y., Dai, Z. G., & Lu, T. 2003, *ApJ*, 592, 347
- Zhang, S. N., Cui, W., & Chen, W. 1997, *ApJ*, 482, L155